ELSEVIER

Materials Science and Engineering A223 (1997) 179–185

MATERIALS SCIENCE & ENGINEERING A

The mechanical stabilisation of Widmanstätten ferrite

P.H. Shipway*, H.K.D.H. Bhadeshia

University of Cambridge/JRDC, Department of Materials Science and Metallurgy, Pembroke Street, Cambridge CB2 3QZ UK

Abstract

Mechanical stabilisation is a phenomenon in which displacive transformation is retarded when it occurs from a parent phase which is plastically deformed. Compression experiments, in which plastically deformed austenite was allowed to transform to Widmanstätten ferrite, have revealed that like bainite and martensite, Widmanstätten ferrite is also susceptible to mechanical stabilisation. The amount of Widmanstätten ferrite that could be obtained decreased when the austenite was deformed, as growth became hindered by the accumulated debris of dislocations in the austenite. The microstructure nevertheless became refined as the number density of nucleation sites was increased by the deformation process. Severe deformation eventually led to a recovery in the maximum attainable quantity of Widmanstätten ferrite, because of an overriding effect of the increased nucleation rate. The results are shown to be consistent with the growth of Widmanstätten ferrite occurring by a displacive mechanism. © 1997 Elsevier Science S.A.

Keywords: Invariant-plain strain; Widmanstätten ferrite; Steel; Transformation

1. Introduction

Widmanstätten ferrite grows at high temperatures by a paraequilibrium mechanism in which the plates of ferrite lengthen at a rate which is controlled by the diffusion of carbon in austenite. It is nevertheless a displacive transformation because the change in lattice is accomplished by the coordinated motion of iron and substitutional atoms. This coordinated motion causes the shape of the transformed region to change, the shape deformation being an invariant-plane strain (IPS) with a large shear component [1]. The diffusion of carbon does not contradict this displacive character because interstitials can move without affecting the shape change, the substitutional lattice still being displaced into its new structure [2]. There is a large strain energy associated with such shape deformations [3], but Widmanstätten ferrite can nevertheless form at very low undercoolings below the equilibrium transformation temperature. This is because the plates tend to grow in pairs consisting of two adjacent invariant-plane strains which mutually accommodate and hence reduce the strain energy [1,4,5]. Surface relief is often observed following the growth of Widmanstätten ferrite [6,7], and has been described as tent-like [8].

The association of a mechanism of transformation with any phase has consequences on the way in which the kinetics and thermodynamics of formation of that phase can be estimated. One of these for a displacive mechanism is that the interfacial structure should be glissile dislocations whose motion is impeded by obstacles of the kind which interfere with normal slip processes. One way in which this effect manifests itself is the phenomenon of mechanical stabilisation. It is well-established that heavy deformation of austenite prior to its transformation hinders the growth of martensite, leading to a smaller fraction of overall transformation, even though its heterogeneous nucleation rate is increased in correspondence with the larger defect density. [9–13]. Thus, whereas an appropriate stress can stimulate displacive transformation in the same way that it enables normal deformation [14,15], mechanical stabilisation actually retards the displacive decomposition of the austenite. Recent work [16] has shown that like martensite, bainite can also be mechanically stabilised. The purpose of the present work was to demonstrate a similar mechanical stabilisation effect for Widmanstätten ferrite, thus giving a greater confidence in the favoured interpretation of its mechanism of transformation. We also wished to complete the demonstration that all the ferrite transformation prod-

* Corresponding author. Department of Materials Engineering and Materials Design, University Park, Nottingham, NG7 2RD, UK

PII S0921-5093(96)10479-2

ucts which cause an IPS shape change of the type described earlier show this unique mechanical stabilisation characteristic of a displacive transformation mechanism.

2. Experimental method

2.1. Test material

The alloy used for this work was Fe–0.059C–1.96Si–2.88Mn–0.1Ni wt.%. The material was homogenised at 1250°C for 72 h in a pure argon atmosphere in a sealed quartz tube and then quenched in water to ensure uniform composition of the starting material.

Cylindrical specimens (8 mm diameter by 12 mm length) were machined for straining in uniaxial compression. Friction between the cylinder faces and the test machine platens is expected to cause barrelling of the cylinder, so that the degree of strain in the sample will be a function of location, as shown by a finite-element-model (FEM) calculation (Fig. 1). The diagram is illustrative; the actual strains depend on flow stress, work hardening rate, strain rate sensitivity and platen-workpiece friction coefficient. However, it indicates the wide range of strains expected to occur in such a test. In this case, the longitudinal true strain is -0.69, but there are regions close to the platen face where the effective strains are not much greater than -0.1 (the 'dead zone') and there are regions in the centre where the effective strain is close to -1.0. The strain decreases along the axis of compression from the specimen centre to the platen face, and also decreases away from the centre towards the specimen edge in a direction normal to the compression axis. Such variations in strain should be reflected in microstructural changes within any given specimen; the extent of transformation can be followed using microhardness measurements.

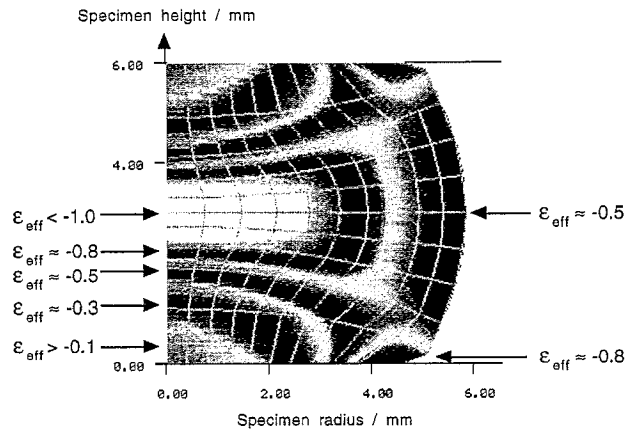

Fig. 1. FEM calculation of strains in a cylinder of initial height 12 mm and radius 4 mm when compressed to final height of 6 mm with interfacial friction coefficient of 0.5. (Half cylinder shown). Values of strain contours are as indicated. Calculation made using Deform, a commercially available FEM package.

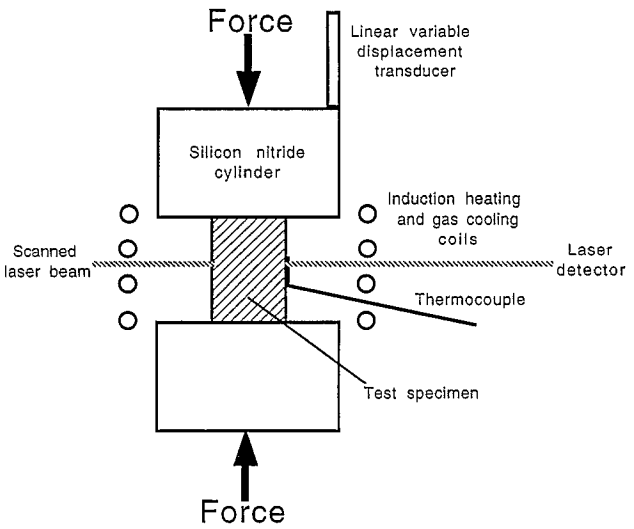

Fig. 2. A schematic diagram for the apparatus used for thermo-mechanical testing.

2.2. Thermomechanical testing

Thermomechanical treatments were carried out using an adapted Thermecmastor Z simulator which allowed control of sample temperature, uniaxial load and strain. Fig. 2 shows a schematic diagram of the experimental arrangement. The sample was heated by induction in a high vacuum ($\sim 4 \times 10^{-2}$ Pa). A Pt-PtRh (Type R) thermocouple was attached centrally to the sample surface; in another experiment, the measured temperature variation along the sample length was established to be less than ± 10°C. The sample was cooled at the desired rate using helium gas. Helium is used in preference to nitrogen in order to achieve higher cooling rates and more accurate control. Deformation was applied using a servo-hydraulic system, with either load or displacement control of the ram position. The system is capable of applying loads of up to 55 kN, the load being applied via silicon nitride cylinders.

The sample temperature, load, time and longitudinal displacements were measured concurrently. The strain was detected using a linear variable displacement transducer (LVDT).

The temperature at which Widmanstätten ferrite was the dominant product of isothermal transformation was determined heuristically to be 545°C. At 560°C, little Widmanstätten ferrite was formed, even after extended periods, (Fig. 3) whereas at 545°C a sizeable volume fraction was formed (Fig. 4). Samples were thus deformed to varying degrees between 560 and 600°C in the austenitic condition, after treatment at 1200°C. The

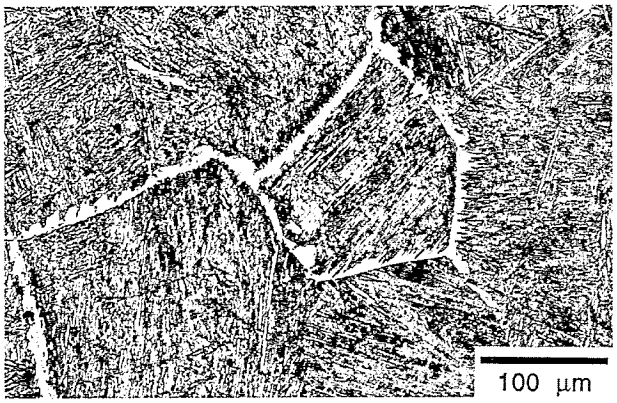

Fig. 3. Microstructure of the core region of a sample following austenization, isothermal hold at 560°C for 3600 s and subsequent quenching. Only a small amount of Widmanstätten ferrite is observed.

deformation was followed by isothermal transformation to Widmanstätten ferrite at 545°C. Fig. 5 illustrates the thermo-mechanical treatments, together with the time periods involved.

All the deformations were achieved at constant velocity rather than constant strain rate, and were applied over a 5 s period regardless of the magnitude of the final strain. Following sample deformation, the position of the crosshead was switched to load control, and the growth of Widmanstätten ferrite occurred with an applied longitudinal compressive stress of ~ 1 MPa, the minimum necessary to allow the longitudinal strain to be monitored throughout the transformation. Matsuzaki et al. [17] have shown that this compressive stress has a negligible effect on the bainite reaction, and it is assumed that this is also the case for the decomposition to Widmanstätten ferrite. In all cases (except where explicitly stated), the isothermal transformation time was sufficient to allow the reaction to stop. Following the transformation, the sample was gas quenched to room temperature.

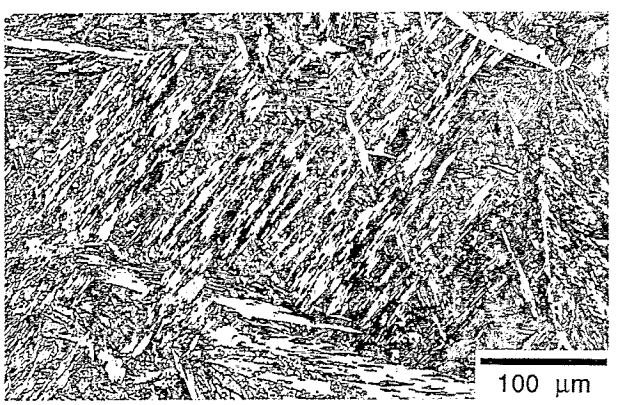

Fig. 4. Microstructure of the core region of a sample following austenization, isothermal hold at 545°C for 3600 s and subsequent quenching. A significant amount of Widmanstätten ferrite (the lighter phase) is observed.

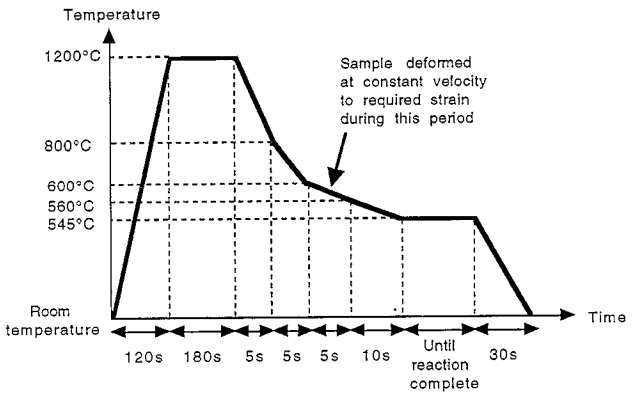

Fig. 5. Thermal and mechanical cycles of the test series.

Optical metallography was conducted on meridional plane sections of the cylindrical samples. Microhardness tests were performed using a Leitz Miniload tester with a Vickers pyramidal indenter and an indenting force of 4.903 N. The load chosen was a compromise allowing indentations to be placed reasonably close together but also sampling a reasonable area of microstructure (the indentation diagonals were typically between 45 and 55 μm in length). Indentations were made along the compression axis of samples at spacings of 300 μm.

Following indentation, the samples were re-ground and polished and etched with a 2% nital solution for optical microscopy.

3. Results and discussion

The engineering-stress/true-strain relationship for the deformation of austenite at 600°C (Fig. 6) is approxi-

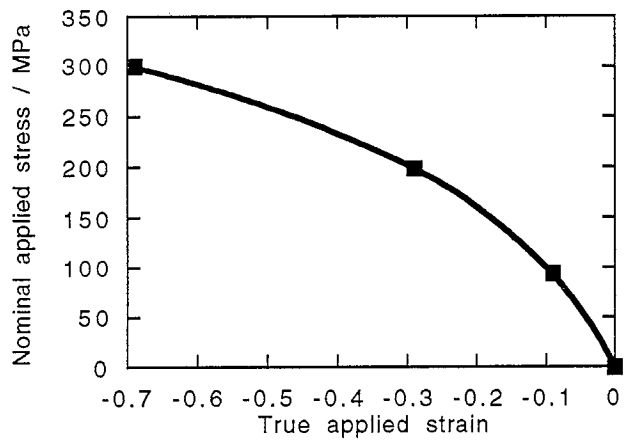

Fig. 6. Maximum nominal applied stress as a function of total applied longitudinal true strain for samples deformed in 5 s in the temperature range 600–560°C (Fig. 5).

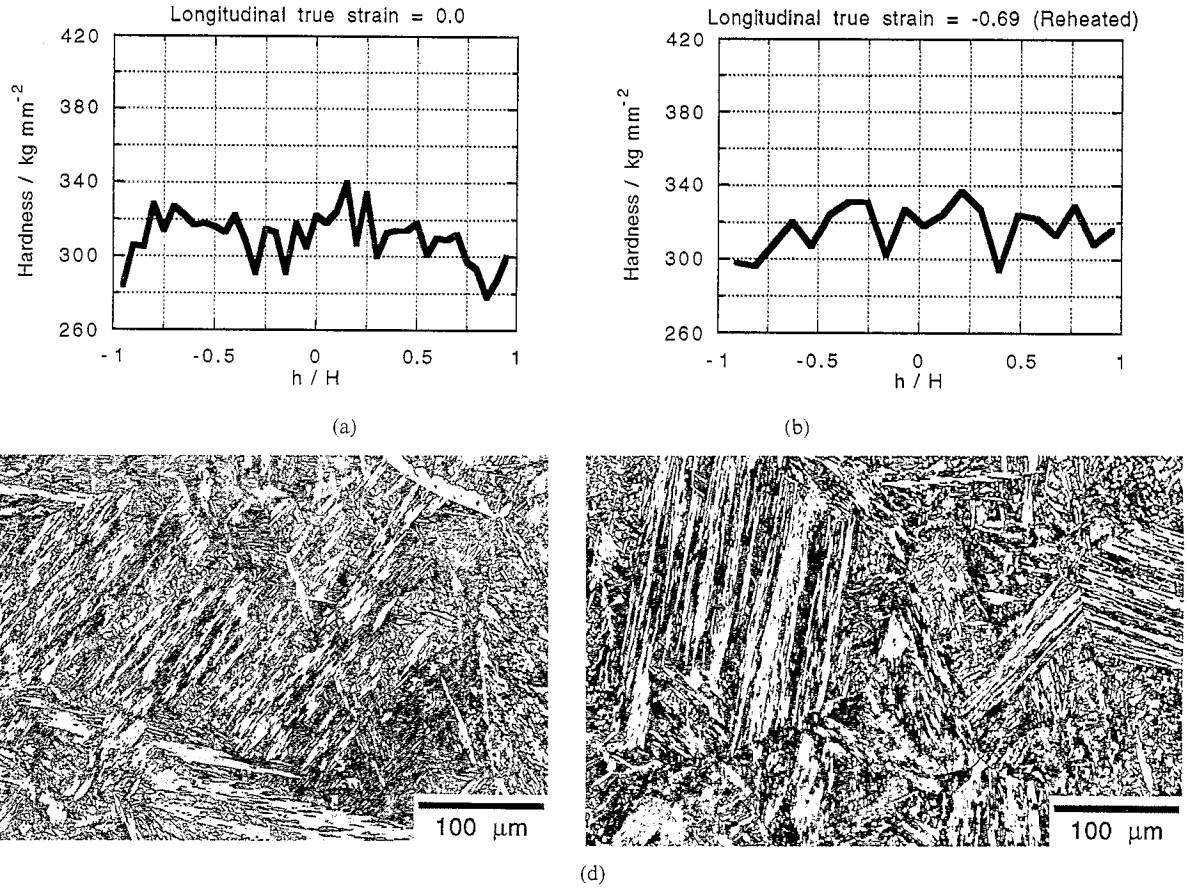

Fig. 7. Hardness profiles along the specimen axis of samples, and corresponding microstructures, resulting from the following thermo-mechanical cycles. (a) Thermal cycle of Fig. 5, with no deformation. H, cylinder half height; h, distance from centre of specimen. (b) Specimen heated and cooled to 560°C with an applied longitudinal true strain of -0.69. Then reheated to 1200°C for 180 s and from there following the thermal cycle of Fig. 5 with no further deformation. H, cylinder half height; h, distance from centre of specimen. (c) Microstructure of the core region of the sample corresponding to Fig. 7(a). (d) Microstructure of the core region of the sample corresponding to Fig. 7(b).

mately parabolic as might be expected from the usual work hardening models.

As discussed earlier, the deformation of austenite resulted in barrelled specimens. There is a small possibility that the radio frequency (RF) induction furnace used may lead to a non-uniform heating of the sample during the isothermal transformation to bainite. A sample was thus deformed to a longitudinal true strain of -0.69 before being reheated to 1200°C for 180 s, so that a severely barrelled sample with undeformed austenite could then be transformed to Widmanstätten ferrite in the way described previously to check for inhomogeneous heating effects. Fig. 7(a) and (b) show the hardness profiles along the axis of the sample transformed at 545°C with no deformation and the sample transformed following deformation and reaustenisation; Fig. 7(c) and (d) show the corresponding micrographs. There clearly is no perceptible effect of the shape of the specimen per se on the development of transformation.

Fig. 8 shows the hardness profiles along the axis of specimens that were deformed prior to transformation. A higher hardness generally indicates less isothermal transformation product and thus more martensite. Comparison with Fig. 7(a) shows that all the samples have rather higher hardnesses in the central regions where the plastic deformation has been large. The effect is pronounced even for an applied longitudinal true strain of only -0.09 (Fig. 8(a)) and remains so for an applied strain of -0.29 (Fig. 8(b)). However, the suppression of growth of Widmanstätten ferrite appears to become less pronounced at the applied longitudinal true strain is raised to -0.69 (Fig. 8(c)).

However, examination of the microstructures from the 'dead zones' and highly deformed central regions (Fig. 9) clearly reveals the effect of deformation on the transformation. Fig. 9(a), (c) and (e) show the microstructure in the dead zones of the samples given increasing overall strains. Each of these structures are similar to each other. They are finer and show greater extent of transformation than the microstructure of the central region of an undeformed specimen, probably due to the lower temperatures in the specimen close to the silicon nitride platen due to heat transfer from the

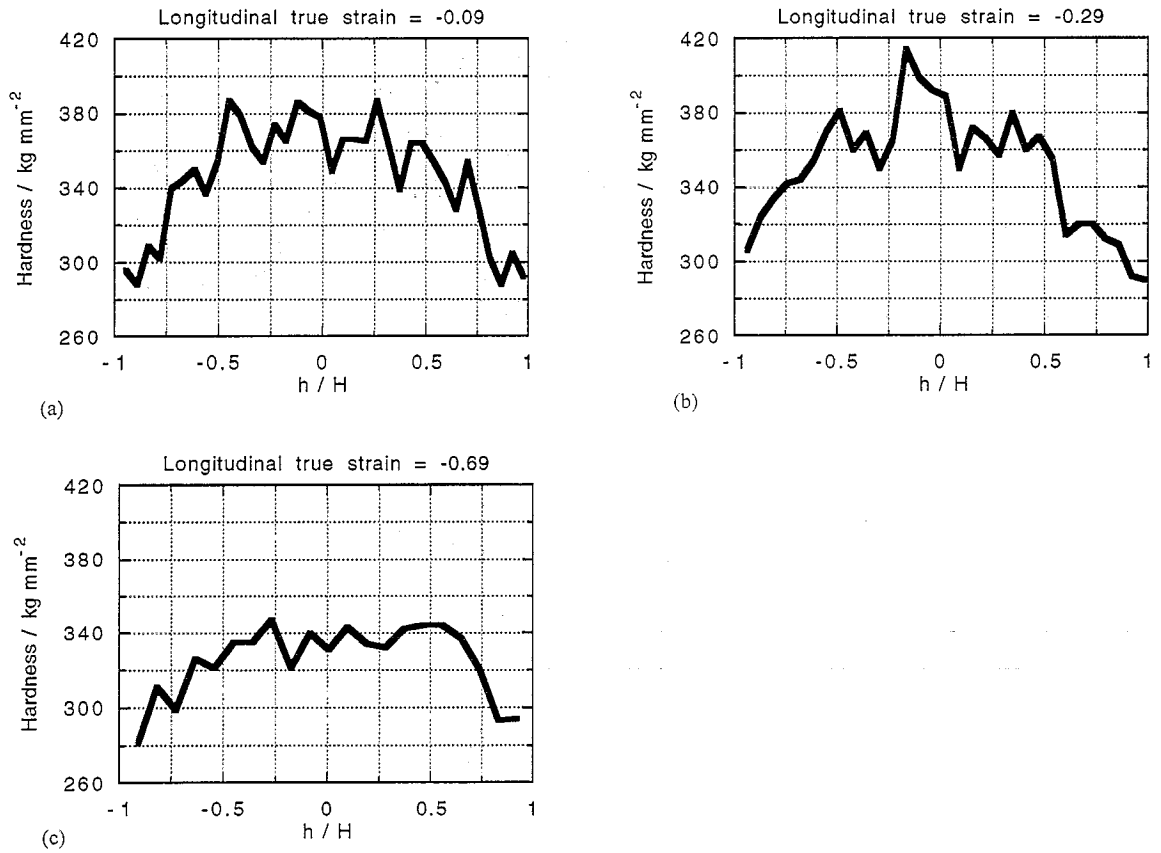

Fig. 8. Hardness profiles along the specimen axis of samples following the thermo-mechanical cycle shown in Fig. 5 with various applied longitudinal true strains. H, cylinder half height; h, distance from centre of specimen. (a) -0.09, (b) -0.29, (c) -0.69.

specimen to the latter. The microstructures from the central regions of these deformed specimens are shown in Fig. 9(b), (d) and (f). Strain of the sample to a value of -0.09 has reduced the volume fraction of Widmanstätten ferrite in the central region of the specimen (Fig. 9(b)); the higher strain of -0.29 has almost entirely prevented the formation of Widmanstätten ferrite, leaving a microstructure composed almost entirely of martensite with some grain boundary ferrite (Fig. 9(d)). A further increase in the applied strain has promoted the formation of a large volume fraction of an isothermal transformation product. This product is likely to be Widmanstätten ferrite as it has a similar appearance and appears to form along curving bands within the grains which were the deformed habit planes within the austenite (Fig. 9(f)).

Deformation of the austenite leads to a large increase in dislocation density. These dislocations hinder the movement of the glissile interface required for the formation of Widmanstätten ferrite, and thus stabilise the austenite. However, a large enough dislocation density appears to act as a further nucleation source for Widmanstätten ferrite, leading to the fine microstructure of Fig. 9(f). Thus, in the same way as for the formation of bainite and martensite, formation of Widmanstätten ferrite is suppressed by the presence of dislocations in the transforming austenite, indicating that Widmanstätten ferrite does indeed form by a similar displacive mechanism to bainite and martensite.

Fig. 10 shows the hardness profile along the axis of a specimen that was deformed to a longitudinal true strain of -0.69, but only held at 545°C for 500 s (rather than the 3600 s hold to ensure the reaction had stopped, Fig. 8(c)). The hardness is generally higher for the sample which had only a short isothermal hold as expected, as less isothermal product has formed, leaving more austenite to transform to martensite. However, the profile shows a deep trough in the central highly deformed region, where hardnesses are of similar magnitude in the samples transformed for 500 and 3600 s. Fig. 11(a) and (b) shows micrographs of the 'dead zone' and highly deformed central region of the sample given the short isothermal hold respectively (cf. Fig. 9(e) and (f)). Much less Widmanstätten ferrite has formed in the dead zone at 500 s than at 3600 s. However, the microstructures in the central regions are very similar at the two times. Increasing the nucleation site density and thus allowing more plates to grow increases the kinetics of formation of Widmanstätten ferrite; as the plate size increases, the rate of transformation decreases.

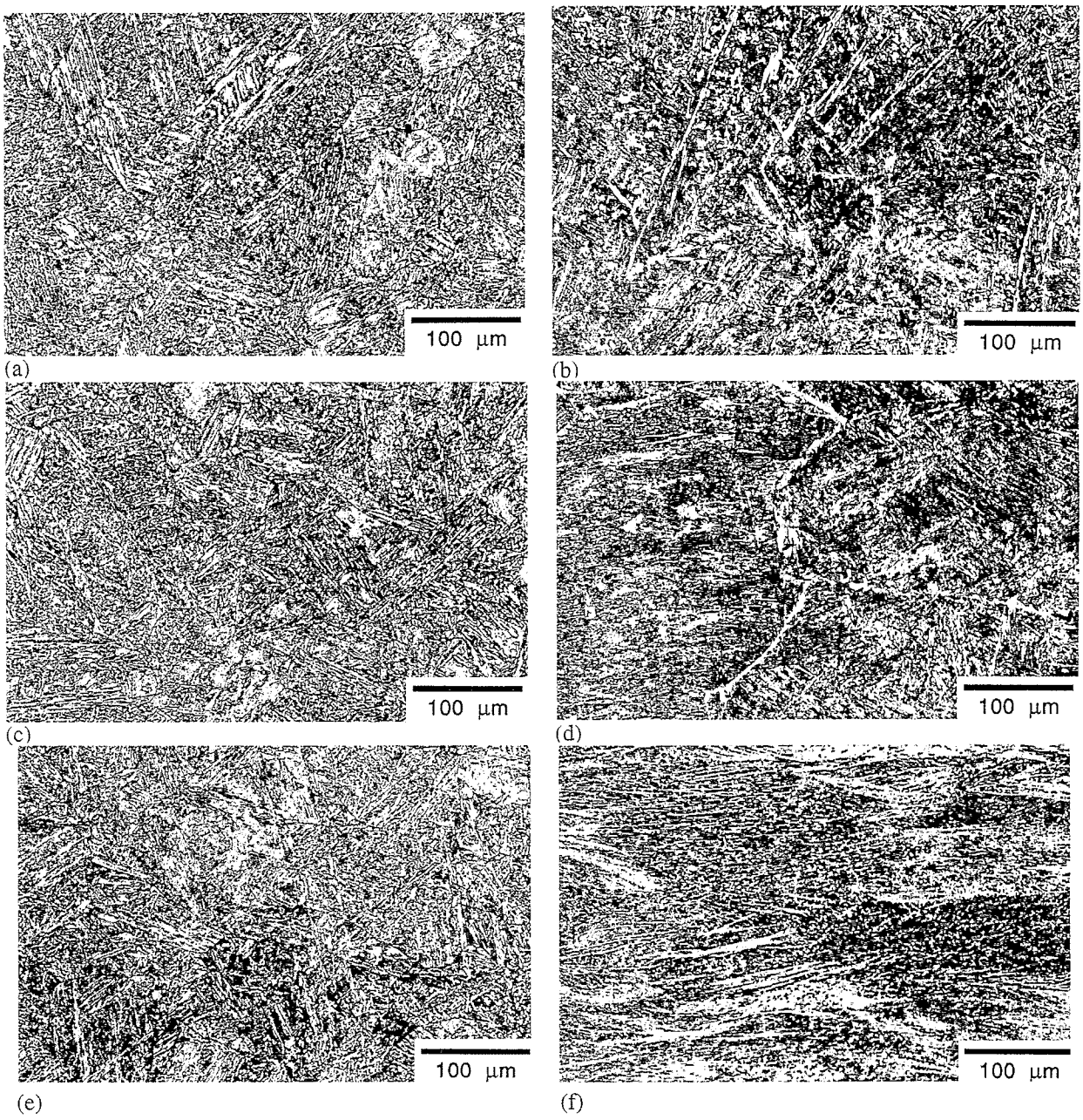

Fig. 9. Micrographs of the Widmanstätten ferrite microstructures formed after thermo-mechanical treatment of Fig. 5. (a) The dead zone - longitudinal true strain = −0.09. (b) The core region–longitudinal true strain = −0.09. (c) The dead zone–longitudinal true strain = −0.29. (d) The core region–longitudinal true strain = −0.29. (e) The dead zone–longitudinal true strain = −0.69. (f) The core region–longitudinal true strain = −0.69.

4. Conclusions

Experiments have shown that the growth of Widmanstätten ferrite is retarded in plastically deformed austenite, consistent with its displacive transformation mechanism. The deformation of austenite prior to its transformation also leads to an increase in the number density of nucleation sites, leading to a refinement of microstructure. For severe deformations, the large increase in the number density of nuclei is found to revive the extent of transformation to Widmanstätten ferrite, albeit to a finer microstructure.

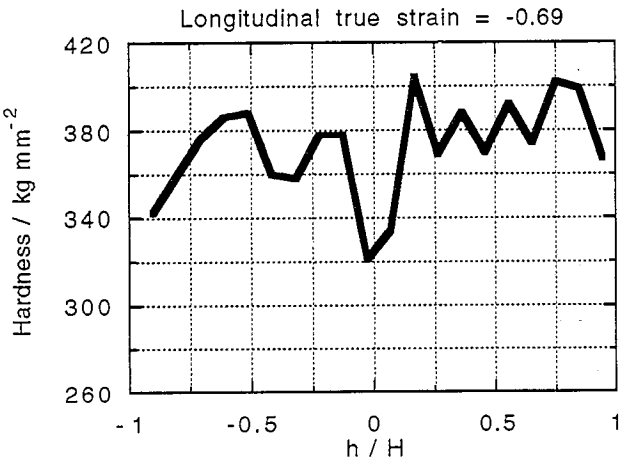

Fig. 10. Hardness profile along the specimen axis of a sample following the thermo-mechanical cycle shown in Fig. 5 with an applied longitudinal true strains of -0.69. The isothermal hold time at 545°C was only 500 s. H, cylinder half height; h, distance from centre of specimen.

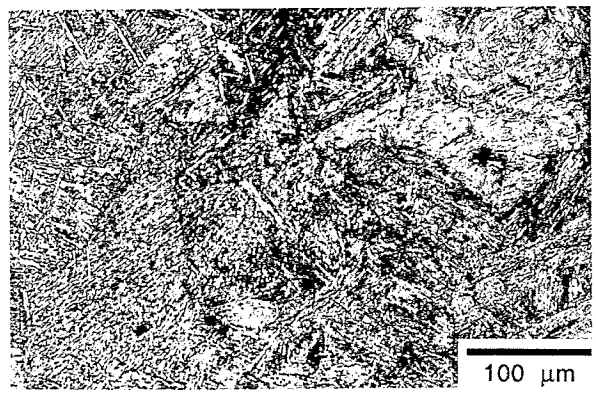

(a)

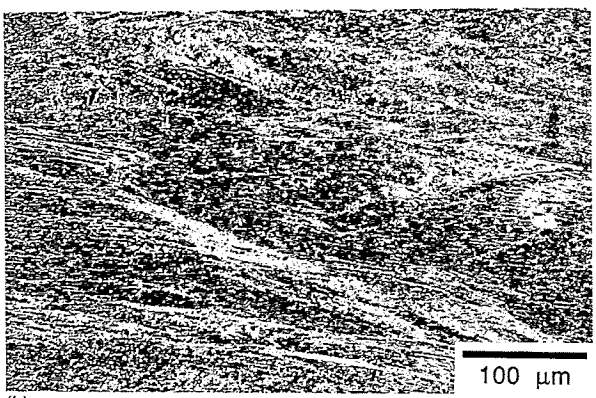

(b)

Fig. 11. Micrographs of the Widmanstätten ferrite microstructures formed after thermo-mechanical treatment described in Fig. 10. (a) The dead zone, (b) the core region.

When the transformation data for steels are considered together, it is clear that martensite, bainite and Widmanstätten ferrite, all of which cause an invariant-plane strain shape deformation, are susceptible to mechanical stabilisation. This is in contrast to reconstructive transformations (such as the formation of allotriomorphic ferrite), which are always found to be accelerated by plastic deformation of the parent phase.

Acknowledgements

We are grateful to the Engineering and Physical Science Research Council and to the 'Atomic Arrangements: Design and Control Project' (a collaborative venture between the Research and Development Corporation of Japan and Cambridge University) for supporting this work. We also thank Professor Colin Humphreys for the provision of laboratory facilities at the University of Cambridge and Dr S.M. Roberts for assistance with finite-element-modelling.

References

[1] J.D. Watson and P.G. McDougall, *Acta Metall.*, *21* (1973) 961–973.
[2] J.W. Christian, in V.F. Zackay and H.I. Aaronson (eds.), *Decomposition of austenite by diffusional processes*, Interscience, NY, 1962, p. 371–386.
[3] J.W. Christian, *Acta Metall.*, *6* (1958) 377–379.
[4] H.K.D.H. Bhadeshia, *Acta Metall.*, *29* (1981) 1117–1130.
[5] H.K.D.H. Bhadeshia, *Scr. Metall.*, *14* (1980) 821–824.
[6] Y. Ohmori, H. Ohtsubo, K. Georgima and N. Maruyama, *Mater. Trans. JIM*, *34* (1993) 216–223.
[7] S. Okaguchi, H. Ohtani and Y. Ohmori, *Mater. Trans. JIM*, *32* (1991) 697–704.
[8] K.R. Kinsman, E. Eichen and H.I. Aaronson, *Metall. Trans. A*, *6* (1975) 303–317.
[9] E.S. Machlin and M. Cohen, *Trans. AIME*, *191* (1951) 746–754.
[10] H.C. Fiedler, B.L. Averbach and M. Cohen, *Trans. ASM*, *47* (1955) 267–290.
[11] W.C. Leslie and R.L. Miller, *ASM Trans. Q.*, *57* (1964) 972–979.
[12] J.R. Strife, M.J. Carr and G.S. Ansell, *Metall. Trans. A*, *8* (1976) 1471–1484.
[13] V. Raghavan, in G.B. Olson and W.S. Owen (eds.), *Martensite, a tribute to Morris Cohen*, ASM International, Materials Park, 1992, pp. 197–226.
[14] J.R. Patel and M. Cohen, *Acta Metall.*, *1* (1953) 531–538.
[15] J.W. Christian, *Metall. Trans. A*, *13* (1982) 509–538.
[16] P.H. Shipway and H.K.D.H. Bhadeshia, *Mater. Sci. Tech.*, *11* (1995) 1116–1128.
[17] A. Matsuzaki, H.K.D.H. Bhadeshia and H. Harada, *Acta Metall. Mater.*, *42* (1994) 1081–1090.